ISSN 0036-0244, Russian Journal of Physical Chemistry A, 2018, Vol. 92, No. 2, pp. 235–243. © Pleiades Publishing, Ltd., 2018.
Original Russian Text © S.S. Sologubov, A.V. Markin, N.N. Smirnova, N.A. Novozhilova, E.A. Tatarinova, A.M. Muzafarov, 2018, published in Zhurnal Fizicheskoi Khimii, 2018, Vol. 92, No. 2, pp. 219–227.

Thermodynamic Properties of a First-Generation Carbosilane Dendrimer with Terminal Phenylethyl Groups

S. S. Sologubov[a], **A. V. Markin**[a,*], **N. N. Smirnova**[a], **N. A. Novozhilova**[b],
E. A. Tatarinova[b], **and A. M. Muzafarov**[c]
[a] *Lobachevsky State University, Nizhny Novgorod, 603950 Russia*
[b] *Enikolopov Institute of Synthetic Polymeric Materials, Russian Academy of Sciences, Moscow, 117393 Russia*
[c] *Nesmeyanov Institute of Organoelement Compounds, Russian Academy of Sciences, Moscow, 119991 Russia*
**e-mail: markin@calorimetry-center.ru*

Received March 30, 2017

Abstract—The heat capacity of a first-generation carbosilane dendrimer with terminal phenylethyl groups as a function of temperature in the range from 6 to 520 K is studied for the first time via precision adiabatic vacuum calorimetry and differential scanning calorimetry. Physical transformations, such as low-temperature structural anomaly and glass transition are detected in the above-mentioned range of temperatures, and their standard thermodynamic characteristics are determined and analyzed. The standard thermodynamic functions of the studied dendrimer in the range of $T \to 0$ to 520 K are calculated from the experimental data, as is the standard entropy in the devitrified state at $T = 298.15$ K. The standard thermodynamic characteristics of the carbosilane dendrimers studied in this work and earlier are compared.

Keywords: carbosilane dendrimers, adiabatic vacuum calorimetry, differential scanning calorimetry, heat capacity, glass transition, thermodynamic functions

DOI: 10.1134/S0036024418010260

INTRODUCTION

A new and rapidly developing field of modern polymer chemistry is synthesizing and studying the properties of a specific class of high-molecular-weight compounds: dendrimers, which are nanosized spherical macromolecules characterized by a regular hyperbranched three-dimensional architecture and surface layer functionality [1–7]. Dendrimers have good solubility in most organic solvents, along with low viscosity of solutions, compared to linear polymers with equivalent molecular weights. Due to their unique structure, dendrimers are capable of self-assembly [8].

There are currently several ways of synthesizing dendrimers (divergent, convergent, and combined methods) that allow controlled increases in the molecular weights of compounds, their size, and the number of terminal functional groups on their outer layers [9]. The nature of these groups plays a key role in different properties of dendrimers.

The different chemical natures of dendrimer molecules provide many promising prospects for their practical application. Dendrimers are used effectively in designing modern nanomaterials with a wide spectrum of unique properties [10]. Carbosilane dendrimers are characterized by thermodynamic and kinetic stabilities, due to the low polarity and high strength of Si–C bonds [11]; this allows their use in preparing catalysts of chemical reactions [12]. Due to their biological inertness and low toxicity, dendrimers are often used in biomedicine as well [13–15].

The study of standard thermodynamic characteristics of dendrimers in a wide range of temperatures via precision adiabatic vacuum calorimetry (AVC) and differential scanning calorimetry (DSC) has allowed the detection and analysis of certain changes of practical significance in the properties of compounds, depending on their compositions and structures [16–25].

This work is a continuation of our study of the thermodynamic properties of carbosilane dendrimers with different terminal functional groups. The aims of this work was to study the heat capacity of a first-generation carbosilane dendrimer with terminal phenylethyl groups as a function of temperature in the range of 6 to 520 K via calorimetry; to detect possible physical transformations in the abovementioned range of temperatures, and to determine their thermodynamic characteristics; to calculate the standard thermodynamic functions (heat capacity $C_p^o(T)$, enthalpy $[H^\circ(T) - H^\circ(0)]$, entropy $[S^\circ(T) - S^\circ(0)]$, and the Gibbs function $[G^\circ(T) - H^\circ(0)]$) for the range of $T \to$ 0 to 520 K, along with standard entropy of formation $\Delta_f S^\circ$ of the dendrimer in the devitrified state at $T = 298.15$ K; and to compare the thermodynamic

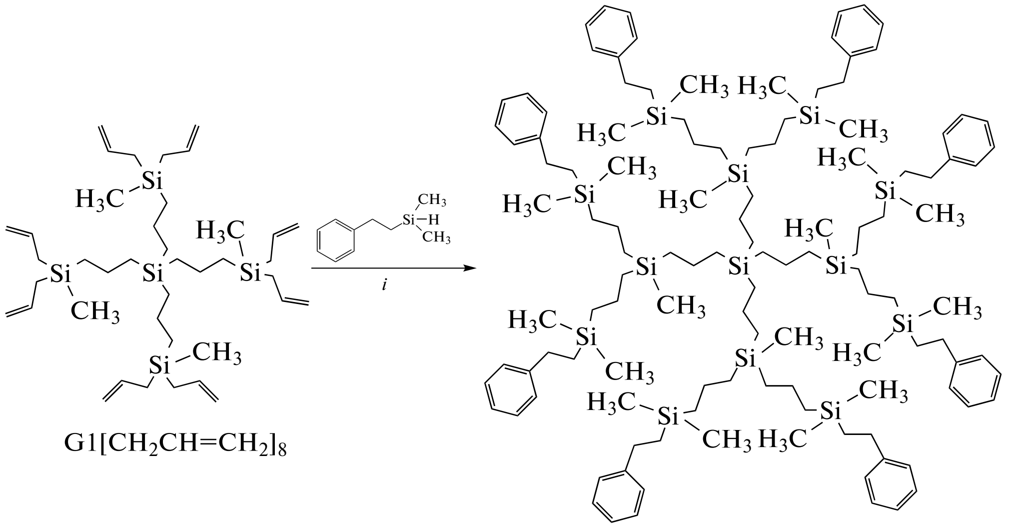

G1[CH$_2$CH=CH$_2$]$_8$

G1[CH$_2$CH$_2$C$_6$H$_5$]$_8$

Fig. 1. Synthesis scheme and structure of a first-generation carbosilane dendrimer with terminal phenylethyl groups G1[CH$_2$CH$_2$C$_6$H$_5$]$_8$; *i* is the Karstedt catalyst in toluene.

characteristics of the dendrimers studied in this work and earlier.

EXPERIMENTAL

Characteristics of the Investigated Sample

Figure 1 shows the synthesis scheme and structure of our carbosilane dendrimer. G1 is the number of the dendrimer's generation, and the structural formula in square brackets specifies the fragment of the terminal group of the dendrimer's surface layer.

Our dendrimer sample was synthesized at the Enikolopov Institute of Synthetic Polymeric Materials, Russian Academy of Sciences, according to the procedure described in [26]. Under normal conditions, dendrimer G1[CH$_2$CH$_2$C$_6$H$_5$]$_8$ is a clear, colorless, viscous liquid.

The composition and structure of the compound were confirmed via elemental analysis and ^{1}H NMR spectroscopy. Found (%): C, 71.95; H, 10.01; Si, 18.08. Calculated (%): C, 71.63; H, 10.22; Si, 18.15. ^{1}H NMR (CDCl$_3$), δ: −0.08 (s, 12 H, CH$_2$Si(C$\underline{H}_3$)CH$_2$CH$_2$CH$_2$Si); −0.03 (s, 48 H, CH$_2$CH$_2$CH$_2$Si(C$\underline{H}_3$)$_2$CH$_2$CH$_2$); 0.51–0.60 (m, 48 H, SiC$\underline{H}_2$CH$_2$C$\underline{H}_2$Si); 0.80–0.87 (m, 16 H, Si(CH$_3$)$_2$C$\underline{H}_2$CH$_2$C$_6$H$_5$); 1.25–1.38 (m, 24 H, SiCH$_2$C$\underline{H}_2$CH$_2$Si); 2.55–2.62 (m, 16 H, CH$_2$C$\underline{H}_2$C$_6$H$_5$); 7.11–7.28 (m, 40 H, C$\underline{H}$ (arom)).

The dendrimer was purified by chromatographic methods. The content of the main substance in the sample was more than 99 mol %. The molecular weight of the dendrimer (molecular formula, $C_{120}H_{204}Si_{13}$) was calculated using the standard atomic weights table recommended by the IUPAC [27].

Apparatus and Measuring Procedures

The heat capacity of the studied dendrimer in the range of 6 to 344 K was measured using a fully automated BKT-3 adiabatic vacuum calorimeter (Termis, Russia). The instrument design and measurement procedures were described in detail in [28, 29].

The calorimetric ampule was a thin-walled cylindrical titanium vessel with a volume of 1.5 cm^3. The ampule with the investigated substance was filled at room temperature with high-purity helium acting as the heat exchange gas. The cooling agents were liquid helium and nitrogen.

The BKT-3 device was calibrated by measuring the heat capacity of the calorimetric system with an empty ampule. The operational reliability of the calorimeter was verified by measuring the C_p^o values of reference samples of high-purity copper, corundum, and benzoic acid. The calorimetric device and the measuring procedure allowed us to determine the heat capacities of substances with an error of no more than ±2% in the range of 6–15 K; ±0.5% in the range of 15–40 K; and ±0.2% in the range of 40–350 K. The errors in measuring the temperature and enthalpies of different transformations were ±0.01 K and ±0.2%, respectively.

The heat capacity in the range of 344 to 520 K was measured using a DSC 204 F1 Phoenix differential scanning calorimeter (NETZSCH Gerätebau, Germany). The design and operating principle of the calorimeter were described in [30, 31].

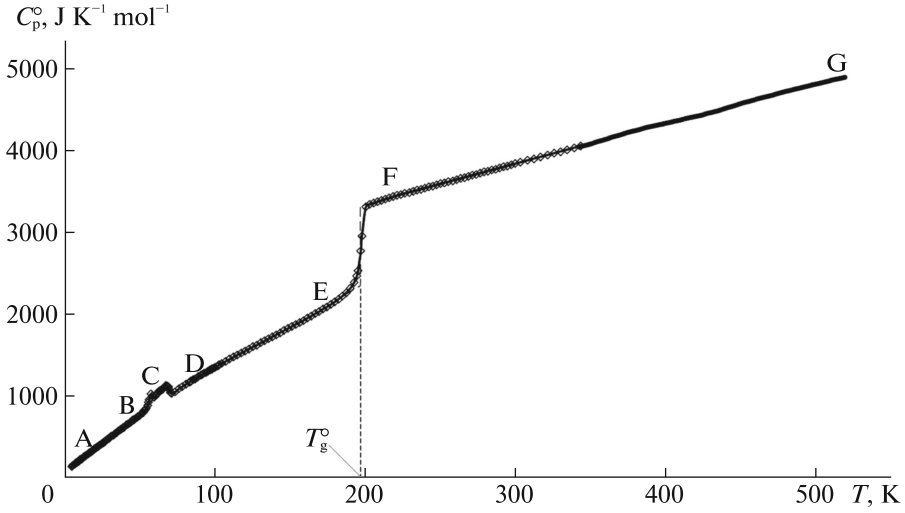

Fig. 2. Heat capacity of the $G1[CH_2CH_2C_6H_5]_8$ carbosilane dendrimer as a function of temperature. AE is an amorphous (glassy) state; FG is an amorphous (devitrified) state; BCD is the apparent heat capacity in the range of the anomaly; and T_g^o is the glass transition temperature.

The operational reliability of the calorimeter was verified by standard calibration experiments to determine the thermodynamic characteristics of the melting of indium, tin, bismuth, zinc, mercury, potassium, cesium chloride, and biphenyl. The apparatus and the measuring procedure allowed us to determine the temperatures and enthalpies of physical transformations with errors of ±0.5 K and ±1%, respectively.

To determine the C_p^o values of the studied dendrimer, three sequential measurements of the baseline, reference sample (corundum), and the dendrimer sample were made in an argon atmosphere. The rate at which the ampule containing the substance was heated was 5 K/min. The procedure for determining the C_p^o values from the DSC measurement data was described in detail in the NETZSCH Proteus software. A comparison between the measured heat capacity of corundum and the corresponding literature data revealed the error in the C_p^o values for our substances: ±2%.

RESULTS AND DISCUSSION

Heat Capacity

The heat capacity of the $G1[CH_2CH_2C_6H_5]_8$ carbosilane dendrimer as a function of temperature in the range of 6 to 520 K is shown in Fig. 2. The experimental C_p^o values for the studied compound are given in Table 1. The weights of dendrimer test portions loaded into the BKT-3 and DSC ampules were 0.1880 and 0.0243 g, respectively. The heat capacity of the studied dendrimers was 25–60% of the total heat capacity of the calorimetric ampule with the substance. The experimental C_p^o values in the investigated range of temperatures where there were no transformations were smoothed using power and semilogarithmic polynomial equations; the corresponding coefficients were selected using special computer programs.

Anomaly

The studied sample of the carbosilane dendrimer $G1[CH_2CH_2C_6H_5]_8$ was cooled from room temperature to the initial temperature of measurement ($T \sim 6$ K) at a rate of 0.02 K/s. The compound was supercooled and vitrified under the conditions of our calorimetric apparatus. With subsequent heating, the heat capacity–temperature curve for the $G1[CH_2CH_2C_6H_5]_8$ dendrimer displayed a low-temperature anomaly consisting of a positive deviation from the normal (interpolated) trend of the $C_p^o = f(T)$ curve (Fig. 3). This anomaly was reproduced each time the sample was cooled and C_p^o was measured. Similar anomalies were observed in the same range of temperatures for carbosilane dendrimers (typically lower than the fifth generation) with other terminal groups [16, 18, 19, 22, 24]. It was found that the detected heat capacity anomaly was due to the vibrational excitation of eclipsed groups of repeating fragments of the dendrimer upon its heating and the freezing of the vibrations when the compound was cooled. According to the McCullough thermodynamic classification [32], the transformations observed in the studied compounds can be attributed to an equilibrium relaxation transition of the order–disorder type.

Table 1. Experimental molar heat capacity [J K^{-1} mol^{-1}] of the G1[$CH_2CH_2C_6H_5$]$_8$ carbosilane dendrimer: $M(C_{120}H_{204}Si_{13})$ = 2011.843 g/mol

T, K	C_p^o	*T*, K	C_p^o	*T*, K	C_p^o	*T*, K	C_p^o	*T*, K	C_p^o	*T*, K	C_p^o
Series 1		28.38	450.1	63.21	1030	128.87	1617	246.04	3553	385.5	4255
5.90	141	29.11	459.4	63.79	1053	131.44	1643	248.66	3566	388.5	4270
6.43	148	29.70	468.2	64.77	1058	134.02	1667	251.34	3580	391.5	4283
6.91	154	30.51	478.2	65.39	1072	136.60	1693	253.97	3593	394.5	4295
7.36	161	31.03	486.4	66.26	1081	139.18	1719	256.60	3605	397.5	4308
7.78	166	31.90	499.5	66.99	1104	141.76	1742	259.23	3618	400.5	4317
8.16	172	32.36	505.1	67.83	1109	144.34	1768	261.85	3631	403.5	4330
8.52	177	33.31	517.8	68.55	1123	146.93	1794	264.48	3644	406.5	4344
8.87	181	33.72	523.5	69.41	1117	149.51	1819	267.11	3657	409.5	4355
9.21	186	34.74	538.3	70.17	1107	152.10	1842	269.73	3670	412.5	4370
9.53	191	35.50	548.5	70.60	1074	154.69	1869	272.35	3683	415.5	4383
9.80	194	36.19	557.5	71.40	1041	157.29	1893	274.98	3696	418.5	4394
10.09	198	36.97	568.8	72.21	1030	159.88	1917	277.60	3709	421.5	4406
10.41	203	37.64	577.6	74.63	1046	162.47	1944	280.21	3722	424.5	4418
10.77	208	38.37	588.0	77.04	1083	165.07	1971	282.83	3735	427.5	4434
11.10	212	39.11	597.5	79.46	1112	167.70	1999	285.44	3748	430.5	4448
11.66	220	39.79	608.2	81.89	1141	170.30	2024	288.04	3761	433.5	4462
12.13	225	40.29	614.1	83.98	1161	172.89	2055	290.64	3774	436.5	4477
12.62	232	40.72	620.1	84.31	1167	175.50	2083	293.25	3787	439.5	4494
13.11	240	41.07	625.5	85.20	1179	178.10	2111	295.84	3799	442.5	4513
13.63	247	42.09	638.7	87.71	1205	180.71	2144	298.42	3812	445.5	4528
13.80	250	43.13	653.5	Series 2		183.32	2177	300.99	3825	448.5	4546
13.98	252	44.14	667.6	86.75	1195	185.92	2215	304.52	3842	451.5	4564
14.60	260	45.00	678.7	89.19	1222	188.53	2258	309.01	3864	454.5	4579
15.21	269	45.49	685.6	90.23	1233	191.15	2308	313.49	3886	457.5	4593
15.85	276.6	46.17	695.0	91.63	1249	193.76	2382	317.94	3909	460.5	4610
16.45	285.8	46.78	703.6	92.76	1259	195.62	2461	322.39	3930	463.5	4625
17.07	293.2	47.26	709.5	94.07	1274	196.36	2523	326.82	3952	466.5	4639
17.67	301.6	48.12	720.3	95.29	1286	198.18	2761	331.24	3974	469.5	4652
18.28	310.9	49.25	734.5	96.52	1299	198.93	2947	335.65	3996	472.5	4666
18.68	316.3	49.96	744.1	97.82	1311	201.46	3295	340.05	4018	475.5	4681
19.17	323.2	50.75	756.2	98.98	1325	204.04	3328	344.43	4039	478.5	4698
19.51	327.8	51.71	771.2	99.15	1327	206.65	3342	Series 3 (DSC)		481.5	4712
19.95	334.0	52.47	782.5	100.35	1337	209.30	3360	343.5	4028	484.5	4725
20.43	341.3	53.17	795.5	101.43	1348	211.92	3375	346.5	4048	487.5	4738
21.05	349.1	53.98	812.8	102.89	1364	214.54	3392	349.5	4061	490.5	4751
21.55	355.8	54.62	824.8	103.25	1368	217.16	3405	352.5	4078	493.5	4765
22.20	364.9	55.50	847.7	103.89	1375	219.78	3422	355.5	4096	496.5	4779
22.77	372.7	56.49	878.6	105.80	1395	222.40	3437	358.5	4111	499.5	4792
23.38	381.1	57.02	916.4	108.35	1421	225.02	3450	361.5	4128	502.5	4804
23.76	386.5	57.45	954.2	110.90	1445	227.65	3465	364.5	4147	505.5	4818
24.59	397.9	58.55	1020	113.45	1471	230.27	3475	367.5	4163	508.5	4832
25.07	404.4	59.21	1001	116.01	1497	232.90	3488	370.5	4178	511.5	4845
25.83	413.9	60.10	979.5	118.58	1520	235.53	3501	373.5	4196	514.5	4858
26.39	422.6	60.60	980.7	121.14	1545	238.15	3514	376.5	4212	517.5	4869
27.10	431.4	61.66	994.5	123.71	1570	240.78	3527	379.5	4227	520.5	4882
27.73	441.0	62.20	1012	126.30	1596	243.41	3540	382.5	4240		

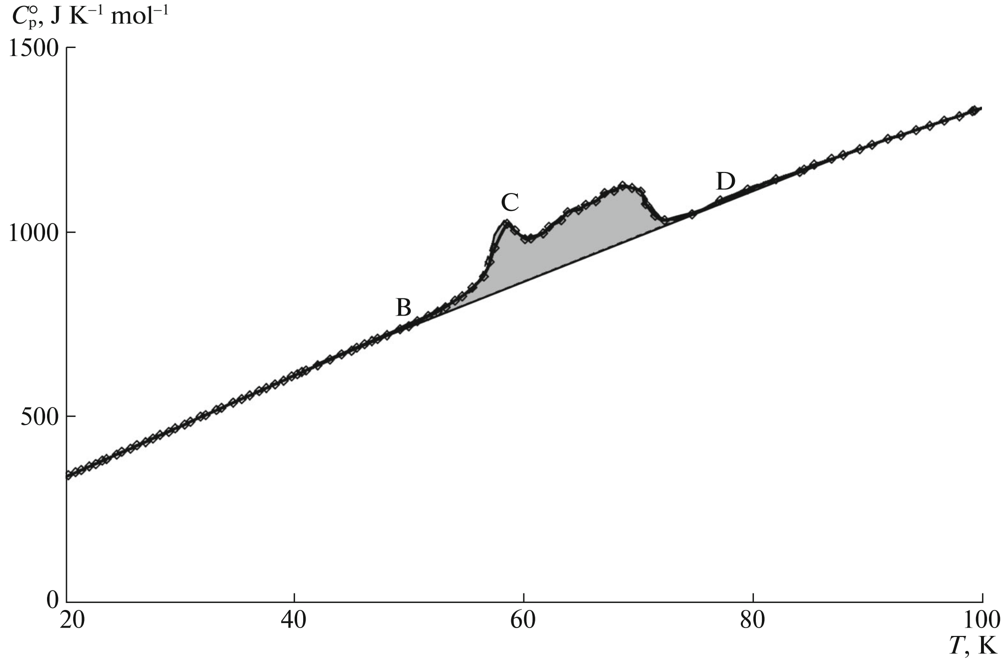

Fig. 3. Low-temperature anomaly of the heat capacity of the G1[$CH_2CH_2C_6H_5$]$_8$ carbosilane dendrimer. BCD is the apparent heat capacity; BD is the normal (interpolated) trend of the heat capacity curve.

The infrared (IR) spectral data of dendrimers in [20] confirmed that the detected anomaly was caused by fine structural changes in lower-generation dendrimers. At $T \approx 60$ K, the terminal groups of dendrimers have low mobility, but the methyl fragments of compounds can display reorientational motions. The occurrence of low-temperature structural anomalies in low-generation dendrimers with different terminal functional groups has a systematic character and does not depend on the nature of the dendrimers' surface layer.

The standard thermodynamic characteristics of low-temperature anomalies in the heat capacities of the G1[$CH_2CH_2C_6H_5$]$_8$ dendrimer and other dendrimers studied earlier are given in Table 2. The anomalies' range of temperatures ΔT was determined graphically. Enthalpy $\Delta_{tr}H°$ was calculated as the difference between the integrals over the apparent and normal (interpolated) heat capacity curves of dendrimer $C_p^o = f(T)$ in the range of anomaly. Entropy $\Delta_{tr}S°$ was calculated in a similar manner from the $C_p^o = f(\ln T)$ curves.

Table 2. Standard thermodynamic characteristics of the low-temperature anomalies of the heat capacities of carbosilane dendrimers with different terminal functional groups

Dendrimer	ΔT, K	$\Delta_{tr}H°$, J/mol	$\Delta_{tr}S°$, J K^{-1} mol^{-1}
G1[$CH_2CH_2C_6H_5$]$_8^*$	53–75	1923 ± 15	27.59 ± 0.33
G3[$CH_2CH_2C_6H_5$]$_{32}$ [22]	49–72	263.5 ± 2.6	3.68 ± 0.05
G1[$CH_2CH{=}CH_2$]$_8^*$ [16]	62–73	414.2 ± 2.5	6.00 ± 0.05
G3[$CH_2CH{=}CH_2$]$_{32}^*$ [16]	55–72	2422 ± 15	35.4 ± 0.4

* The characteristics were calculated per mole of whole macromolecule of dendrimer.

Glass Transition and the Vitreous State

With subsequent heating, the $C_p^o = f(T)$ curve of the G1[$CH_2CH_2C_6H_5$]$_8$ dendrimer exhibited a transformation associated with its glass transition (Fig. 2). The glass transition occurred each time a sample was cooled below the glass transition temperature T_g^o and subsequently heated with repeated measurements of C_p^o. The heat capacity of the studied dendrimer changed smoothly and fairly regularly upon an increase in temperature, with the exception of anomalous regions. The C_p^o values of the dendrimer in the devitrified state grew more slowly when the temperature was raised.

The standard thermodynamic characteristics of the devitrified and glassy states of the G1[$CH_2CH_2C_6H_5$]$_8$ dendrimer and other dendrimers studied earlier are given in Table 3. The interval of the glass transition ΔT and the increase in heat capacity upon the glass transition $\Delta C_p^o(T_g^o)$ were determined graphically. The glass transition temperature T_g^o was calculated according to Alford and Dole [33] from the inflection in the tem-

Table 3. Standard thermodynamic characteristics of the glass transition and glassy state of carbosilane dendrimers with different terminal functional groups

Dendrimer	ΔT	$T_g^\circ \pm 1$	ΔC_p° (T_g°)	$S^\circ(0)$
	K		J K^{-1} mol^{-1}	
$G1[CH_2CH_2C_6H_5]_8^*$	176–215	198	960 ± 10	245 ± 3
$G3[CH_2CH_2C_6H_5]_{32}$ [22]	178–218	199	140 ± 2	36 ± 1
$G6[CH_2CH_2C_6H_5]_{256}$ [22]	178–219	201	129 ± 1	33 ± 1
$G1[CH_2CH{=}CH_2]_8^*$ [16]	150–160	154	406 ± 5	44 ± 1
$G3[CH_2CH{=}CH_2]_{32}^*$ [16]	170–180	173	1610 ± 17	417 ± 5
$G6[CH_2CH{=}CH_2]_{256}^*$ [17]	155–190	180	14250 ± 146	3630 ± 45

* The characteristics were calculated per mole of whole macromolecule of dendrimer.

perature dependence of the dendrimer's entropy of heating $[S^\circ(T)–S^\circ(0)]$. Entropy of configuration S^o_{conf} was calculated using the equation proposed in [34]:

$$S^o_{conf} = \Delta C^o_p(T^o_g)\ln(T^o_g/T_K), \qquad (1)$$

where T_K is the Kauzmann temperature [35] and ratio $(T^o_g/T_K) = 1.29$ [36]. In determining S^o_{conf}, the above relation was assumed to also be true for the compound under study. Since the S^o_{conf} value was close to $S^\circ(0)$, it was logically assumed that $S^o_{conf} = S^\circ(0)$ in determining absolute entropy $S^\circ(T)$ of the dendrimer.

Table 3 shows that dendrimers with terminal allyl groups $GX[CH_2CH{=}CH_2]_z$ devitrify at lower temperatures, compared to those with terminal phenylethyl groups $GX[CH_2CH_2C_6H_5]_z$. The observed difference is quite logical and is due to the higher molecular mobility of the terminal allyl groups in comparison with the phenylethyl groups, which contain low-mobility phenyl fragments.

In [22], we presented a diagram of temperatures of the glass transition T^o_g as a function of generation number of dendrimers. It was found that the glass transition temperature depends more on the nature and structure of terminal groups than on the generation number of dendrimers. In addition, T^o_g ceases to depend on the dendrimer generation number starting with a particular generation (typically the fourth or fifth). The change in the composition and structure of the surface layer of dendrimers is thus an efficient tool for controlling their properties.

Standard Thermodynamic Functions

To calculate the standard thermodynamic functions of the $G1[CH_2CH_2C_6H_5]_8$ dendrimer, its experimental heat capacity values were extrapolated from the initial measurement temperature to $T \to 0$ using the Debye heat capacity function [37]:

$$C^o_p = n\mathbf{D}(\Theta_\mathbf{D}/T), \qquad (2)$$

where $\mathbf{D}$ is the Debye heat capacity function; $n = 3$ and $\Theta_\mathbf{D} = 62.8$ K are specially selected parameters in the range of 7–10 K. The parameters were selected so that Eq. (2) described the experimental C^o_p values of the dendrimer with an error of ±1.5%. In calculating the functions, it was assumed that at $T < 6$ K, Eq. (2) reproduces the C^o_p values of the substance with the same accuracy.

The standard thermodynamic functions of the $G1[CH_2CH_2C_6H_5]_8$ carbosilane dendrimer are given in Table 4. Enthalpies $[H^\circ(T) - H^\circ(0)]$ and entropies $[S^\circ(T) - S^\circ(0)]$ were calculated via numerical integration of the $C^o_p = f(T)$ and $C^o_p = f(\ln T)$ curves, respectively. The Gibbs function $[G^\circ(T) - H^\circ(0)]$ was calculated using the values of the enthalpies and entropies at corresponding temperatures. A similar procedure for calculating standard thermodynamic functions was presented in [38].

The standard entropy of formation $\Delta_f S^\circ$ of the $G1[CH_2CH_2C_6H_5]_8$ dendrimer in the devitrified state at $T = 298.15$ K was calculated using the obtained values of $[S^\circ(T) - S^\circ(0)]$ at the same temperature (Table 4), residual entropy $S^\circ(0)$ (Table 3), and absolute entropies of the elementary substances: C(gr), H_2(g), and Si(cr) [39, 40]. The resulting value $\Delta_f S^\circ(G1[CH_2CH_2C_6H_5]_8) = -(9802 \pm 196)$ J K^{-1} mol^{-1} corresponds to the process

$$120C(gr) + 102H_2(g) + 13Si(cr) \to C_{120}H_{204}Si_{13}(d),$$

where (gr) is graphite, (g) is gas, (cr) is crystal, and (d) is the devitrified state.

Table 4. Standard thermodynamic functions of the $G1[CH_2CH_2C_6H_5]_8$ carbosilane dendrimer: $M(C_{120}H_{204}Si_{13})$ = 2011.843 g/mol

T, K	C_p°	$[S^\circ(T) - S^\circ(0)]$	$[H^\circ(T) - H^\circ(0)]$	$-[G^\circ(T) - H^\circ(0)]$
	$J K^{-1} mol^{-1}$		kJ/mol	
Amorphous (glassy) state				
5	109	51.9	0.184	0.0756
10	197	160	0.984	0.611
15	266	252	2.14	1.65
20	334.5	338.2	3.641	3.124
25	403.3	420.3	5.485	5.021
30	472.2	499.9	7.674	7.322
35	541.2	577.9	10.21	10.02
40	610.4	654.6	13.09	13.10
45	679.0	730.5	16.31	16.56
50	744.5	805.5	19.87	20.40
60	983.2	960.6	28.42	29.21
70	1110	1125	39.10	39.65
80	1123	1267	49.77	51.62
90	1232	1406	61.54	64.99
100	1335	1541	74.36	79.73
110	1437	1673	88.22	95.80
120	1534	1802	103.1	113.2
130	1630	1929	118.9	131.8
140	1726	2053	135.7	151.7
150	1823	2175	153.4	172.9
160	1920	2296	172.1	195.2
170	2022	2416	191.8	218.8
180	2141	2534	212.6	243.6
190	2253	2653	234.6	269.5
198	2348	2748	253.0	291.1
Amorphous (devitrified) state				
198	3308	2748	253.0	291.1
200	3319	2781	259.6	296.6
210	3367	2944	293.0	325.3
220	3424	3102	327.0	355.5
230	3475	3255	361.5	387.3
240	3524	3404	396.5	420.6
250	3573	3549	431.9	455.4
260	3622	3690	467.9	491.6
270	3672	3828	504.4	529.1
280	3721	3962	541.3	568.1
290	3771	4094	578.8	608.4
298.15	3811	4199	609.7	642.2
300	3820	4222	616.8	650.0
310	3869	4348	655.2	692.8
320	3919	4472	694.1	736.9
330	3968	4593	733.6	782.3

Table 4. (Contd.)

T, K	C_p°	$[S^\circ(T) - S^\circ(0)]$	$[H^\circ(T) - H^\circ(0)]$	$-[G^\circ(T) - H^\circ(0)]$
	J K^{-1} mol^{-1}		kJ/mol	
340	4018	4713	773.5	828.8
350	4065	4830	813.9	876.5
360	4122	4945	854.8	925.4
370	4178	5059	896.3	975.4
380	4228	5171	938.4	1027
390	4274	5281	980.9	1079
400	4317	5390	1024	1132
410	4359	5497	1067	1187
420	4402	5603	1111	1242
430	4449	5707	1155	1299
440	4498	5810	1200	1356
450	4551	5911	1245	1415
460	4604	6012	1291	1475
470	4657	6111	1337	1535
480	4706	6210	1384	1597
490	4752	6308	1431	1659
500	4794	6404	1479	1723
510	4835	6499	1527	1787
520	4885	6594	1576	1853

The errors of the calculated function values are 2, 0.5, 0.2, and 2% for C_p^o, 2.3, 0.8, 0.6, and 2.3% for $[S^\circ(T) - S^\circ(0)]$, 2.2, 0.7, 0.5, and 2.2% for $[H^\circ(T) - H^\circ(0)]$, and 3, 1, 0.9, and 3% for $[G^\circ(T) - H^\circ(0)]$ in the range of temperatures of 6–15, 15–40, 40–350, and 350–520 K, respectively.

ACKNOWLEDGMENTS

This work was financially supported by the RF Ministry of Education and Science, project no. 4.5706.2017/BCh; by the Russian Foundation for Basic Research, project nos. 15-03-02112 a and 16-33-00713 mol_a; and by the Russian Science Foundation, project no. 16-13-10521.

REFERENCES

1. D. A. Tomalia, H. Baker, J. Dewald, et al., Polym. J. **17**, 117 (1985).
2. C. J. Hawker and J. M. J. Fréchet, J. Am. Chem. Soc. **112**, 7638 (1990).
3. J.-P. Majoral and A.-M. Caminade, Chem. Rev. **99**, 845 (1999).
4. A. W. Bosman, H. M. Janssen, and E. W. Meijer, Chem. Rev. **99**, 1665 (1999).
5. G. R. Newkome, E. He, and C. N. Moorefield, Chem. Rev. **99**, 1689 (1999).
6. A. M. Muzafarov and E. A. Rebrov, J. Polym. Sci. A: Polym. Chem. **46**, 4935 (2008).
7. A. M. Muzafarov, N. G. Vasilenko, E. A. Tatarinova, G. M. Ignat'eva, V. M. Myakushev, M. A. Obrezkova, I. B. Meshkov, N. V. Voronina, and O. V. Novozhilov, Polymer Sci., Ser. C **53**, 48 (2011).
8. S. C. Zimmerman and L. J. Lawless, Top. Curr. Chem. **217**, 95 (2001).
9. S. M. Grayson and J. M. J. Fréchet, Chem. Rev. **101**, 3819 (2001).
10. J. M. J. Fréchet, J. Polym. Sci. A: Polym. Chem. **41**, 3713 (2003).
11. C. Schlenk and H. Frey, Monatsh. Chem. **130**, 3 (1999).
12. D. Astruc, E. Boisselier, and C. Ornelas, Chem. Rev. **110**, 1857 (2010).
13. S. Svenson and D. A. Tomalia, Adv. Drug Deliv. Rev. **57**, 2106 (2005).
14. R. K. Tekade, P. V. Kumar, and N. K. Jain, Chem. Rev. **109**, 49 (2009).
15. S. H. Medina and M. E. H. El-Sayed, Chem. Rev. **109**, 3141 (2009).
16. B. V. Lebedev, M. V. Ryabkov, E. A. Tatarinova, E. A. Rebrov, and A. M. Muzafarov, Russ. Chem. Bull. **52**, 545 (2003).
17. N. N. Smirnova, B. V. Lebedev, N. M. Khramova, L. Ya. Tsvetkova, E. A. Tatarinova, V. D. Myakushev, and A. M. Muzafarov, Russ. J. Phys. Chem. A **78**, 1196 (2004).

18. N. N. Smirnova, O. V. Stepanova, T. A. Bykova, et al., Thermochim. Acta **440**, 188 (2006).
19. N. N. Smirnova, A. V. Markin, I. A. Letyanina, S. S. Sologubov, N. A. Novozhilova, E. A. Tatarinova, and A. M. Muzafarov, Russ. J. Phys. Chem. A **88**, 735 (2014).
20. A. V. Markin, S. S. Sologubov, N. N. Smirnova, et al., Thermochim. Acta **617**, 144 (2015).
21. S. S. Sologubov, A. V. Markin, N. N. Smirnova, et al., J. Phys. Chem. B **119**, 14527 (2015).
22. S. S. Sologubov, A. V. Markin, N. N. Smirnova, et al., J. Therm. Anal. Calorim. **125**, 595 (2016).
23. A. V. Markin, Ya. S. Samosudova, N. N. Smirnova, et al., J. Therm. Anal. Calorim. **105**, 663 (2011).
24. N. N. Smirnova, A. V. Markin, Ya. S. Samosudova, G. M. Ignat'eva, E. Yu. Katarzhnova, and A. M. Muzafarov, Russ. J. Phys. Chem. A **87**, 552 (2013).
25. Ya. S. Samosudova, A. V. Markin, N. N. Smirnova, et al., J. Chem. Thermodyn. **98**, 33 (2016).
26. N. A. Novozhilova, O. A. Serenko, V. I. Roldughin, et al., Silicon **7**, 155 (2015).
27. J. Meija, T. B. Coplen, M. Berglund, et al., Pure Appl. Chem. **88**, 265 (2016).
28. V. M. Malyshev, G. A. Mil'ner, E. L. Sorkin, et al., Prib. Tekhn. Eksp., No. 6, 195 (1985).
29. R. M. Varushchenko, A. I. Druzhinina, and E. L. Sorkin, J. Chem. Thermodyn. **29**, 623 (1997).
30. G. W. H. Höhne, W. F. Hemminger, and H.-J. Flammersheim, *Differential Scanning Calorimetry* (Springer, Berlin, Heidelberg, 2003).
31. V. A. Drebushchak, J. Therm. Anal. Calorim. **79**, 213 (2005).
32. *Physics and Chemistry of Solid State of Organic Compounds,* Ed. by Yu. A. Pentin (Mir, Moscow, 1967) [in Russian].
33. S. Alford and M. Dole, J. Am. Chem. Soc. **77**, 4774 (1955).
34. G. Adam and J. H. Gibbs, J. Chem. Phys. **43**, 139 (1965).
35. W. Kauzmann, Chem. Rev. **43**, 219 (1948).
36. A. B. Bestul and S. S. Chang, J. Chem. Phys. **40**, 3731 (1964).
37. P. Debye, Ann. Phys. (N.Y.) **344**, 789 (1912).
38. B. V. Lebedev, Thermochim. Acta **297**, 143 (1997).
39. J. D. Cox, D. D. Wagman, and V. A. Medvedev, *CODATA Key Values for Thermodynamics* (Hemisphere, New York, 1989).
40. M. W. Chase, Jr., J. Phys. Chem. Ref. Data, Monograph No. 9 **1–2**, 1 (1998).

Translated by K. Utegenov